frontiers in Energy Research

ORIGINAL RESEARCH
published: 16 February 2021
doi: 10.3389/fenrg.2020.637846

RETRACTED: Optimization of Pyrolysis Parameters for Production of Biochar From Banana Peels: Evaluation of Biochar Application on the Growth of *Ipomoea aquatica*

Wei Zun Te[1]*, Kavinesh Nair Manor Muhanin*[1]*, Yu-Ming Chu*[4,5]**, Anurita Selvarajoo*[1]**, Ajit Singh*[2]*, Shams Forruque Ahmed*[3]*, Dai-Viet N. Vo*[6] *and Pau Loke Show*[1]*

[1]Department of Chemical and Environmental Engineering, University of Nottingham Malaysia, Semenyih, Malaysia, [2]School of Biosciences, University of Nottingham Malaysia, Semenyih, Malaysia, [3]Science and Math Program, Asian University for Women, Chattogram, Bangladesh, [4]Department of Mathematics, Huzhou University, Huzhou, China, [5]Hunan Provincial Key Laboratory of Mathematical Modeling and Analysis in Engineering, Changsha University of Science and Technology, Changsha, China, [6]Center of Excellence for Green Energy and Environmental Nanomaterials (CE@GrEEN), Nguyen Tat Thanh University, Ho Chi Minh City, Vietnam

RETRACTED

OPEN ACCESS

Edited by:
Su Shiung Lam,
University of Malaysia Terengganu, Malaysia

Reviewed by:
Nguyen Thi Dong Phuong,
University of Science and Technology, The University of Danang, Vietnam
C. K. Cheng,
Universiti, Malaysia Pahang, Malaysia
M. Shahabuddin,
Federation University Australia, Australia

***Correspondence:**
Yu-Ming Chu
chuyuming@zjhu.edu.cn
Anurita Selvarajoo
Anurita.Selvarajoo@nottingham.edu.my
Pau Loke Show
showpauloke@gmail.com

Specialty section:
This article was submitted to Bioenergy and Biofuels, a section of the journal Frontiers in Energy Research

Received: *04 December 2020*
Accepted: *23 December 2020*
Published: *16 February 2021*

Citation:
Te WZ, Muhanin KNM, Chu Y-M, Selvarajoo A, Singh A, Ahmed SF, Vo D-VN and Show PL (2021) Optimization of Pyrolysis Parameters for Production of Biochar From Banana Peels: Evaluation of Biochar Application on the Growth of Ipomoea aquatica. *Front. Energy Res. 8:637846. doi: 10.3389/fenrg.2020.637846*

Banana peels waste can be utilized to produce high quality biochar that can be incorporated into the soil for sustainable production of crops. This research analyzed several properties of the biochar produced from the banana peel at different temperatures, residence times and heating rates. This study focuses on the biochar yield and the EDX analysis of the biochar produced. Response surface methodology using central composite design (CCD) was used to optimize these parameters in the batch reactor pyrolysis system. These factors were operated in different ranges for banana peels, in which pyrolysis temperature (200 to 600°C), residence time (60 to 180 min) and heating rate (5 to 15°C·min^{-1}) were varied using 20 experiments respectively. Quality of the biochar was determined based on the biochar yield and O/C ratio. The optimum biochar chosen from the CCD model was applied to several pots of *Ipomoea aquatica* in different biochar dosage levels of 0, 3, 9 and 15 g (0, 1, 3 and 5 wt% of soil) respectively. Pot experiment was conducted with completely randomized design (CRD) of one factor with five replications to correlate the average plant heights with the biochar dosage levels. Results showed that biochar dosage of 1% yields the highest average final *Ipomoea aquatica* plant height of 37.04 cm.

Keywords: pyrolysis, biomass, biochar, banana peel, response surface methodology, completely randomized design

INTRODUCTION

Malaysia is currently under the development of newly industrialized economy, where agricultural field serves as the backbone of this economy even since a long time ago (Abu Darhak, 2015). The intensified agricultural and industrial activities produce various wastes that cause negative impacts to the environment. Agriculture field serves as one of the main contributors to the production of biomass from harvested yields. Biomass is a natural organic renewable material derived from plants and animals (Eia.gov., 2020). Biomass can cause environmental impact such as emission of greenhouse gases (GHG) and pollution of surface water and groundwater if not properly managed and treated. Therefore, concern on the management of these biomass has been arising and many ways have been developed to convert this waste into energy. Recently, production of biochar through slow pyrolysis of biomass is being practised in Malaysia, albeit not fully commercialized.

Bananas are among the most important food crops in terms of production value, with global annual production of around 98 million tonnes. These are commonly grown in small scale by farmers in tropics and sub-tropics throughout more than 150 countries such as countries in Africa, Asia-Pacific and Caribbean and Latin American regions. In Malaysia, there are several banana species that are commonly grown in small-scale, including red bananas, *Raja* banana, Dwarf Orinoco, Kerala bananas, cavendish and plantains (Tan, 2014). Due to the large production of bananas, banana peels wastage has been a major concern since they are generally discarded and disposed to municipal landfills, bringing about environmental pollution.

There are other biomass sources in Malaysia, including but not limited to, dedicated biomass crops, forest residue, manure, municipal solid wastes (MSW), wood waste, and other agricultural waste like coconut husk, rice straw and sugarcane (Nbs 2020.gov.my., 2019). Various thermal conversion methods have been studied and developed to convert the biomass as valuable feedstock into useful products. For instance, biomass has been combusted in the presence of air to obtain heat or electricity, while the residue can be used as soil fertilisers (Selvarajoo et al., 2019). This method is commonly used in agricultural field in Malaysia to improve soil health through direct combustion in which holes are dug on the ground for carbonization process. Nevertheless, this method is not environmentally friendly as it releases large amount of carbon dioxide that contributes to the increase in greenhouse gases (Lawal et al., 2020). Biomass gasification is another process developed to utilize the biomass in which the lignocellulosic materials of the biomass are left to react with gasifying agents like CO_2 to generate combustible gas mixture (Morin et al., 2016). On the other hand, liquefaction of biomass converts it into liquid hydrocarbon mixture that usually generates solid residues and gaseous by-products (Selvarajoo et al., 2019).

Pyrolysis has been widely researched in current times due to its efficient thermal conversion and green technology (Suman and Gautam, 2018). The process can be categorized into three types, which are slow, flash and fast pyrolysis that yields three types of products including biochar, bio-oil and syngas (Selvarajoo et al., 2019). The compositions and yields of the end products are highly dependent on the operating parameters during the pyrolysis process (Rodriguez et al., 2020). Slow pyrolysis utilizes low temperature and heating rate and long residence time and converts most of the biomass into biochar as the moisture and volatile compounds from the biomass are removed, leaving porous structure that contains the aromatic compound and the chemical functional group of the biochar (Lee et al., 2017). The properties of biomass affect its suitability to be pyrolyzed to produce biochar (Veiga et al., 2020). These can be determined using various analyses such as proximate analysis and ultimate analysis. Proximate analysis is used to determine the content of moisture, ash, volatile and fixed carbon in biomass, while the elemental composition of the biomass and biochar are determined using ultimate analysis. For instance, low amount of sulphur and nitrogen in the biomass makes it safe to be used as pyrolysis feedstock. Typically, the concentration of sulphur and nitrogen of less than 1% respectively in the biomass denotes that the biomass is environmentally friendly and pyrolysis of the biomass will not cause major environmental issues (Zainal et al., 2016).

Biochar is a complex solid residue consists of mainly carbon, hydrogen, oxygen and inorganic matters, and is highly beneficial in promoting the agricultural productivity (Morin et al., 2016). The properties of biochar make it suitable to be used as a soil enhancer that improves the soil fertility. Biochar has high carbon content, which contributes to the soil carbon content and improves the soil fertility when applied directly into soil. Biomass depletes atmospheric carbon dioxide through photosynthesis (Osman et al., 2016). Hence a long-term carbon sink will be formed when there is large conversion of biomass to soil carbon species with long half-life (Osman et al., 2016). As a soil enhancer, biochar is capable of retaining water and nutrients in the soil. Biochar is also used in other applications such as energy source, pollutant adsorbent, and carbon sequestration (Xie et al., 2020). Due to its wide range of application, slow pyrolysis has been done on many types of agricultural wastes such as almond shell, corn leaves, corn straw, cotton stalks (Danish et al., 2015), fruit peels including jackfruit peels, lemon peels and orange peels (Pathak et al., 2017), pinewood and timothy grass (Nanda et al., 2014).

There have been several investigations conducted to determine the potential of banana wastes as precursor of biochar and the potential of the biochar in various applications were also examined. (Kabenge et al., 2018) conducted proximate analysis on biochar produced using banana peels and determined it as adequate slow pyrolysis feedstock due to its high level of ash content, fixed carbon and volatile matter. (Selvarajoo et al., 2019) investigated the potential of biochar of banana peels as solid fuel and tested the properties of the biochar formed at different operating condition for the slow pyrolysis process using artificial neural network (ANN) modelling. It was found that temperature has the most significant impact on banana peels char yield. (Sial et al., 2019) studied the beneficial effect of banana peel biochar on reducing emission of greenhouse gases. Through incubation period of 90 days, it was found that the biochar with large pore surface area was able to reduce CO_2, CH_4 and N_2O emission in soil effectively. However, there is no thorough research on the effect of banana peels biochar dosage on plant growth. Kangkong (*Ipomoea aquatica*) was chosen as the plant to evaluate the application of biochar in agricultural application due to its very high growth rate. Hence, the experimental results can be obtained in a very short amount of time of about 4 weeks. It is also easy to grow and is considered a relatively low-maintenance plant.

This study aims to investigate the properties of biochar by slow pyrolysis for banana peels at different temperatures, heating rates

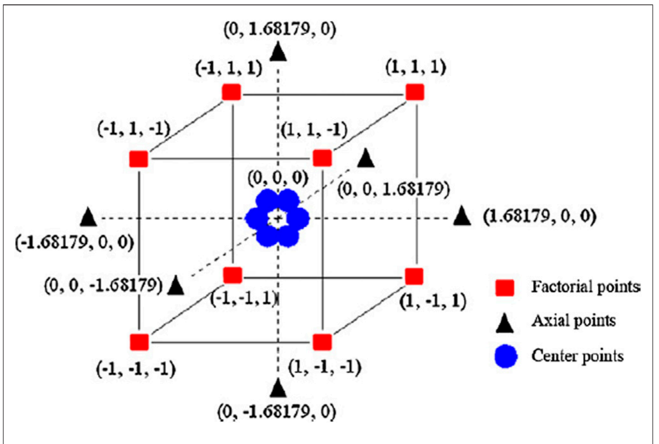

FIGURE 1 | Schematic diagram of a three-factor CCD (Diler and Ipek, 2012).

and residence times. Comprehensive study was done to analyze the properties of biochar from the samples comparing its mass yield and elemental composition by scanning electron microscopy and energy dispersive X-ray spectroscopy (SEM-EDX). Response surface methodology (RSM) with central composite design (CCD) was used to correlate the pyrolysis operating conditions and biochar properties. The optimal biochar with the highest potential in agricultural application was chosen based on pyrolytic properties and biochar yield. Elemental composition of the biochar was used compute the elemental ratio in molar basis that is prominent in determining the suitability of biomass to be utilized in producing biochar through slow pyrolysis process. The optimal biochar was utilized to study the effects of its dosage on the plant height of *Ipomoea aquatica* plant.

MATERIALS AND METHODS

Biomass Sample Preparation

Banana peels were collected from a stall selling banana fritters in Taman Tasik Semenyih, Selangor. These freshly obtained biomass was unfavourable for pyrolysis process due to its high moisture content. This means that much more energy will be dissipated in order to heat up and evaporate the water in the biomass, causing low biochar yield. The banana peels were cut to smaller pieces before being oven-dried at 80°C (Memmert, Germany) to increase the surface area for drying until it reached a moisture content of about 10 wt% on wet basis. The dried biomass was then ground using a miller (Retsch SM 100, Germany) to achieve particle size of ≤5 mm. Smaller particle size in a range of 425 microns to 2 mm was achieved by sieving. Particle size less than 400 microns was undesired as there may be risk of dust explosion during pyrolysis process, and accumulation of dust may cause blockage of pyrolysis reactor outlet (V Birtwistle, 2003).

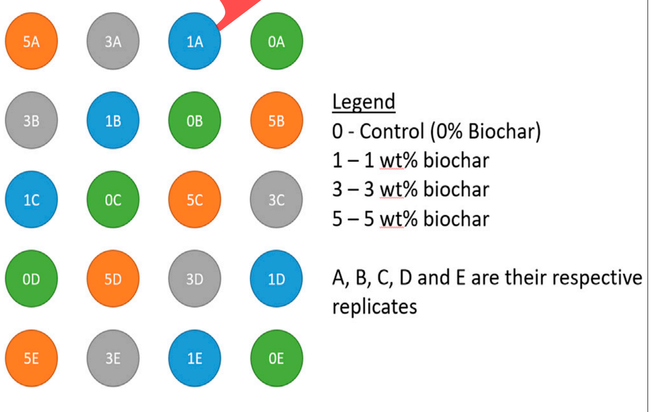

FIGURE 2 | Schematic diagram of the CCD design of the study.

Pyrolysis of Biochar

The dried biomass was pyrolyzed in an electrical horizontal tubular furnace with Carbolite model STF 12/65/550. The customized cylindrical working tube made of stainless-steel acts as the main component of furnace with dimensions of 1,200 mm length, 50 mm inner diameter and 60 mm outer diameter. Thermocouple was installed on the furnace to monitor the temperature of the sample. Nitrogen, N_2, was supplied by a nitrogen tank connected to the working tube through a pipe, with its flow rate set at 50 ml/min and pressure set at 2 bar. Nitrogen was passed through the furnace 10 min before the pyrolysis process as well as during the pyrolysis process to purge the oxygen and prevent the build-up of gaseous product that was formed from reaction. As nitrogen is an inert gas, other undesired reactions can also be prevented during the pyrolysis process. The outlet of the furnace was connected to a conical flask submerged in a water bath, which is a 5 L beaker containing distilled water, to condense and collect the liquid product known as bio-oil. Another conical flask containing silica gel was connected to the sidearm of the first conical flask with a tube to clean the gaseous product that will be discharged into the atmosphere.

20 g of dried biomass was loaded uniformly into a customized stainless-steel sample holder with the dimension of 150 mm length, 40 mm width and 20 mm height for each pyrolysis run. The sample holder was inserted into the middle section of working tube where the heating rate was the most uniform. The connecting flange was sealed with vacuum grease to prevent atmospheric gas from entering the tubular furnace. Each pyrolysis run was conducted after purging at temperature range of 200 to 600°C, residence time of 60 to 180 min and heating rate of 5 to 15°C·min^{-1}. After the completion pyrolysis process, the resulting biochar in the furnace was left to cool until it reached room temperature. The cooled biochar was taken out and weighed to compute the biochar yield using **Eq. 1**.

$$\textit{Biochar Yield}\ (\%) = m/m_o \times 100 \qquad (1)$$

where m is the mass of the biochar produced after pyrolysis, in grams; m_o is the mass of the biomass sample before pyrolysis, in grams.

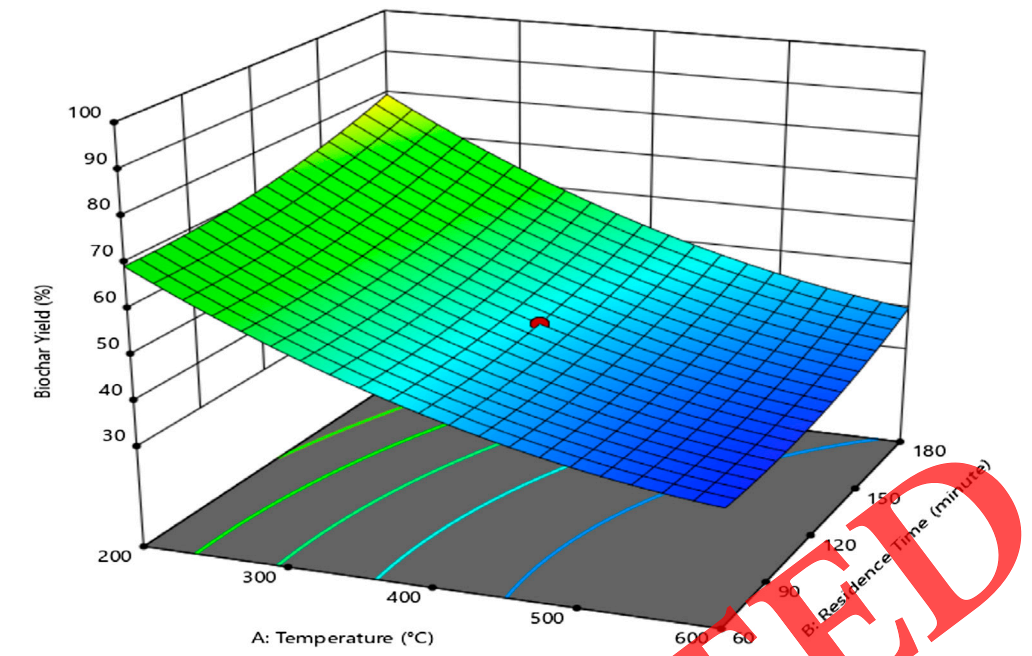

FIGURE 3 | Response surface for biochar yield with varying temperature and residence time at constant heating rate of 10°C·min^{-1}.

Germination and Growing *Ipomoea aquatica* (Kangkong Plants)

Pot culture was utilized to assess the effect of banana peels biochar dosage on the plant height of *kangkong*. *Kangkong* seeds were first germinated in seedling trays filled with peat soil. After the germination at about 7 days, healthy seedlings were carefully removed without damaging the roots and transplanted into pots containing 150 g soil, followed by another 150 g of soil to cover the roots of the plants in the soil. The soil used was laterite soil rich in iron and aluminium. It is abundant in Malaysia, which is a tropical region, and is suitable for planting *kangkong*. The initial plant height was recorded for each plant. 40 ml of water was supplied to each plant when necessary. Fertiliser with nutrient in the ratio of 1:1:1 for N:P:K was dosed into each pot after one week of transplanting. These nutrients were supplied by three different fertilisers, namely urea with 46wt% N, triple super phosphate (TSP) with 45 wt% P, and Muriate of Potash (MOP) with 60 wt% K. It was assumed that 40 kg of each nutrient is required for one hectare of soil, which is approximately equivalent to 2,000,000 kg of dry soil. The required dosage of each fertiliser for each pot (300 g soil) was calculated using **Eq. 2**. From this equation, the dosages of fertilisers per pot were 13.04 mg urea, 13.33 mg TSP and 10 mg MOP. The height of the of plants after germination were recorded each week for 4 weeks. The mean height of kangkong plants with the same biochar dosage were computed each week and its relationship with the biochar dosage was determined using completely randomized design (CRD).

$$\textit{Fertiliser required}\ (\mathrm{kg}) = (100/y) \times 40 \times (0.3/2,000,000) \quad (2)$$

where y is the percentage of the nutrient supplied by the fertiliser.

Analysis of Biochar

The elemental composition of biochar was examined through scanning electron microscope (SEM, Quanta 400F, USA) mounted with an energy dispersive X-ray spectrometer (EDX). The biochar was inserted into the chamber while mounted on SEM stub, at pressure of approximately 1.4×10^{-6} kPa with magnification of 800× and 20,000 accelerating voltages. Each sample was analyzed three times at different locations of the biochar. However, only one spot was chosen and observed for several chosen samples to compare the effect of pyrolysis process parameters on the pore size and surface area. Carbon (C), oxygen (O), sulfur (S), nitrogen (N), phosphorus (P), potassium (K), aluminium (Al), chlorine (Cl), magnesium (Mg) and silicon (Si) composition of the biochar were determined through this method.

Response Surface Methodology

The correlations between the selected inferred properties and the controlled variables in the pyrolysis process were further studied and verified using response surface methodology (RSM), using DesignExpert12 software. This model is an empirical model utilizing collection of mathematical and statistical techniques that utilizes quantitative data to determine regression model that optimize responses affected by several factors. The controlled variable, also known as response or dependant variable, and the manipulated variable, also known as independent variable, can be represented statistically through a three-dimensional space and contours, which help to visualize the response surface (Behera et al., 2018). The mathematical equation of the correlation can also be obtained so that the response can be computed algebraically (Behera et al., 2018). In this study, the selected controlled variables were pyrolysis temperature, heating

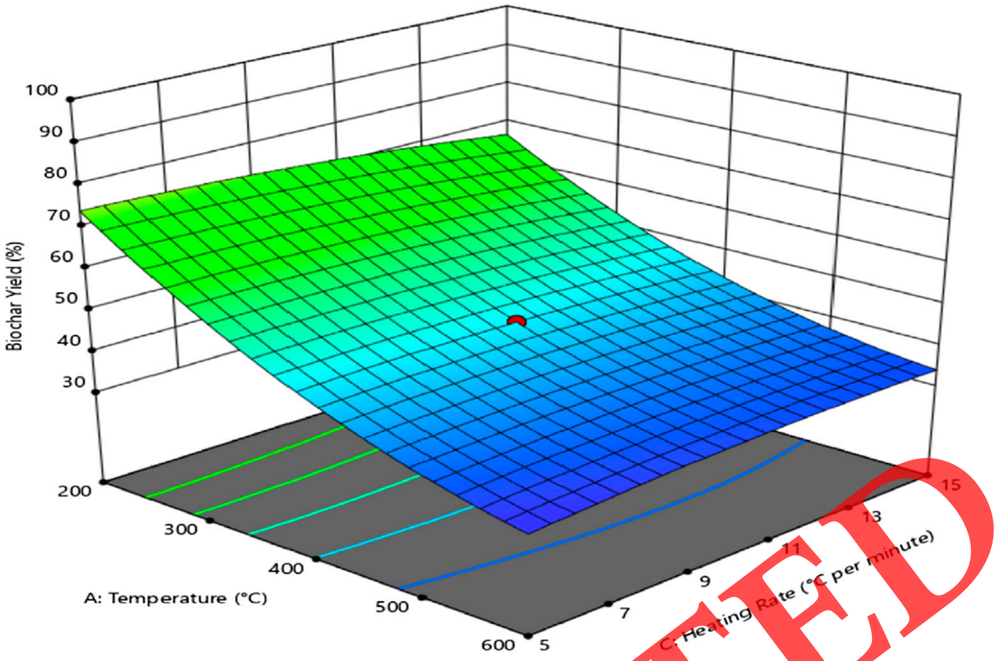

FIGURE 4 | Response surface for biochar yield with varying temperature and heating rate at constant residence time of 120 min.

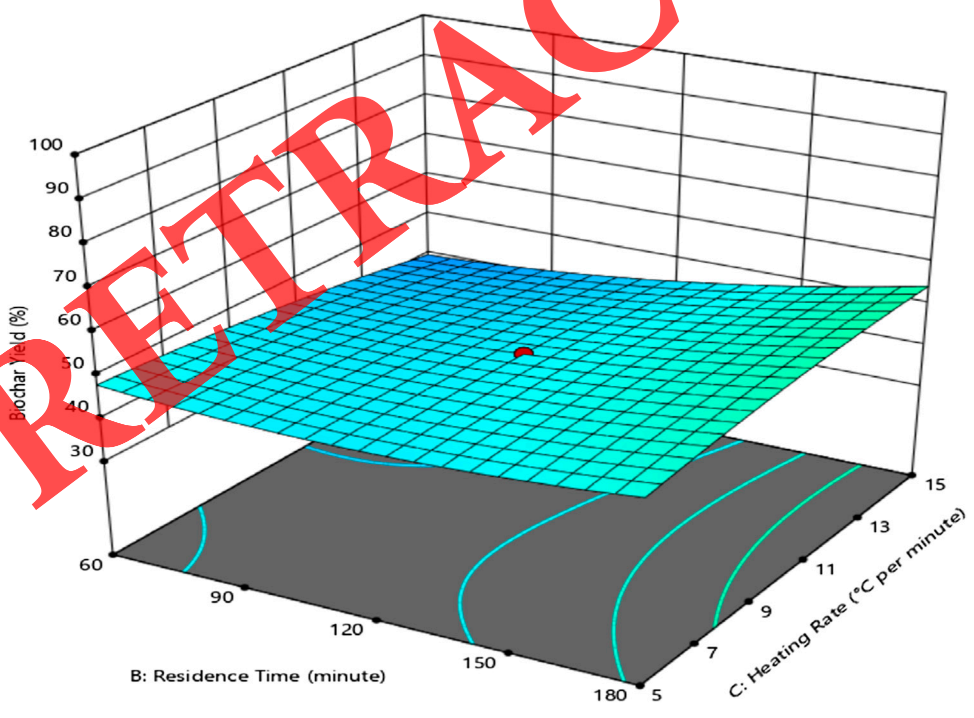

FIGURE 5 | Response surface for biochar yield with varying residence time and heating rate at constant residence time of 400°C.

rate and residence time which are known to affect the yield and properties of biochar. The quality of the biochar was determined by quantifying two parameters of the biochar produced, which are biochar yield and O/C ratio. Biochar yield was calculated using **Eq. 1**, while O/C ratio was computed by dividing the composition of oxygen by the composition of carbon as

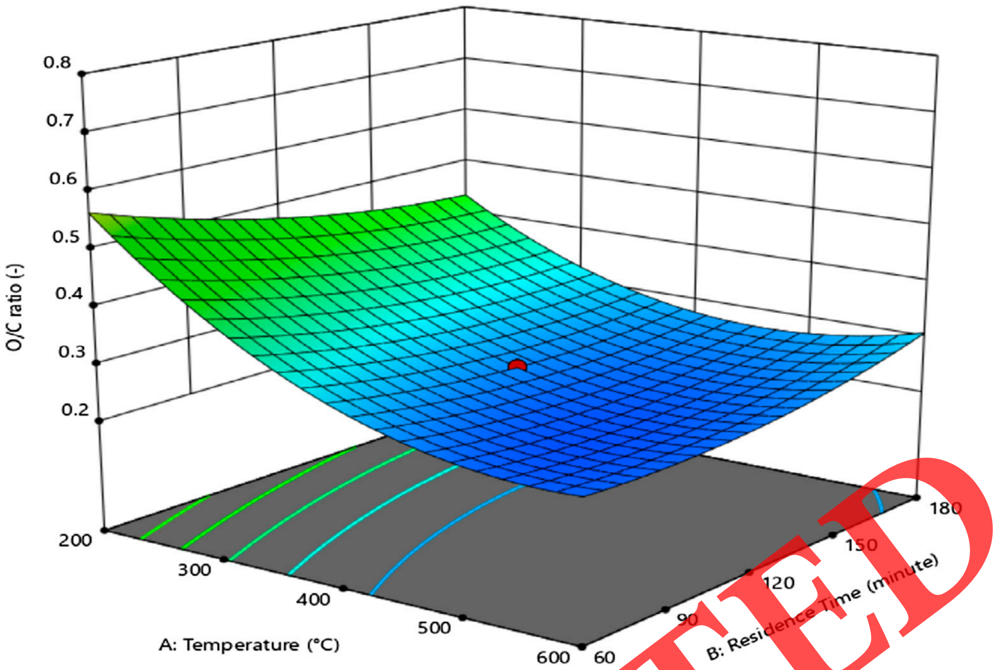

FIGURE 6 | Response surface for O/C ratio with varying temperature and residence time at constant heating rate of 10°C·min^{-1}.

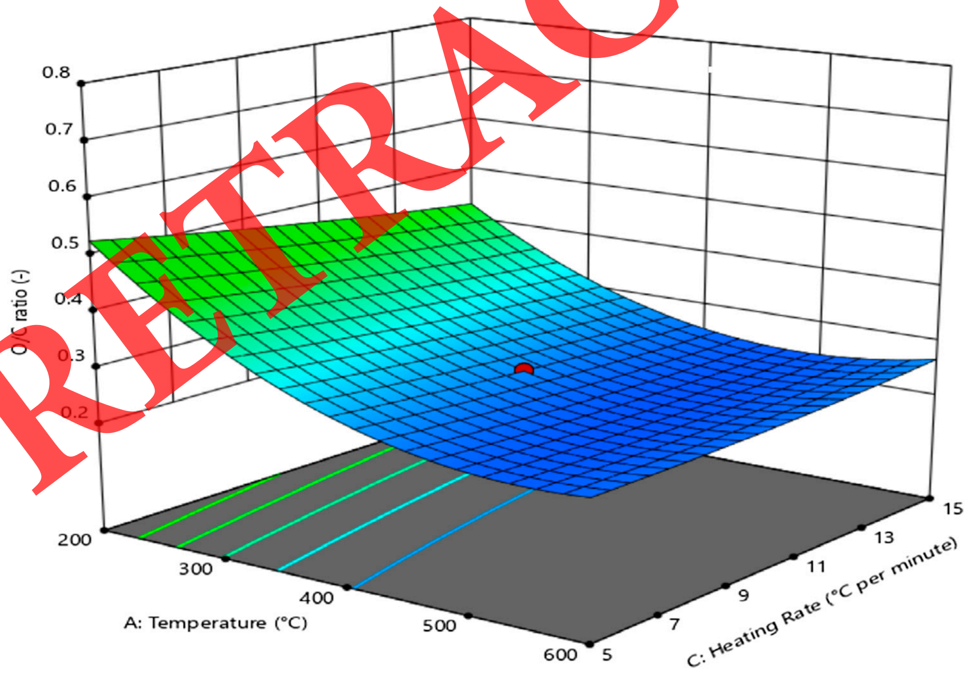

FIGURE 7 | Response surface for O/C ratio with varying temperature and heating rate at constant residence time of 120 min.

determined through the EDX analysis. These parameters were chosen as the response variables to be studied in the modelling.

RSM with central composite design (CCD) is suitable for plotting a quadratic surface with the least number of experiments required, which helps in optimizing the process parameters and developing a relationship between these variables (Montogomery, 2014). It contains an embedded fractional or factorial design with center points and non-centre

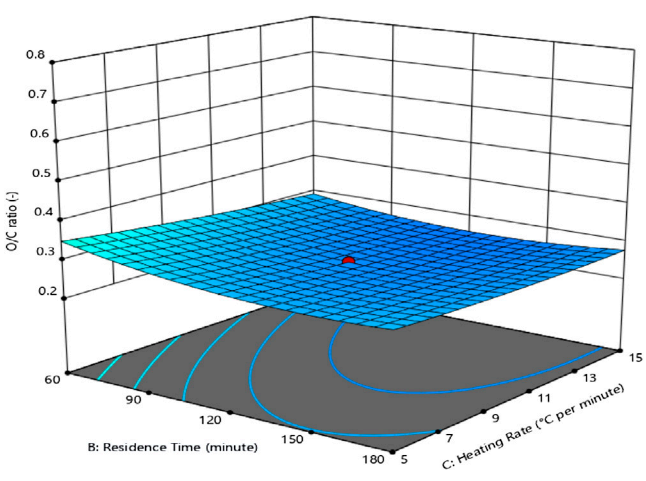

FIGURE 8 | Response surface for O/C ratio with varying residence time and heating rate at constant residence time of 400°C.

points that consists of axial points and factorial points which are useful in estimation of curvature (Itl.nist.gov., 2020). The level of factors in CCD is 5, including upper level, lower level, center point and axial points usually denoted as α, which gives the design flexibility (Olawoye, 2016). Because of this, it is most commonly used for sequential experiment and is therefore suitable for this study. The experiment can be split into sub-fractions that support the two-factor interaction model. For instance, an experimental design can be considered to consist of two blocks if the experiment is carried out at two different locations. In current study, the experimental runs were conducted in a randomised order to eliminate the effect of uncontrolled factors. Considering the only absolute factors that affect the response variables are the three manipulated variables, the modelling of this experiment was assumed to consist of only one block.

In a CCD modelling, 2^n factorial runs, which can include categorical factors and numerical factors, with 2n axial runs are involved (Chung et al., 2018). The center points are plotted to compute the experimental error and determine the adequacy of

TABLE 1 | The coded and uncoded levels of the independent variables.

Terms	Independent variable	Uncoded levels of coded factors				
		Low bound −α (−1.6872)	Low −1	Medium 0	High +1	High bound +α (+1.6872)
A	Temperature	63.6414	200	400	600	736.359
B	Residence time	19.0924	60	120	180	220.908
C	Heating rate	1.59104	5	10	15	18.409

TABLE 2 | Experimental runs for banana peels biochar with independent variables in both coded and actual factors and the respective response, using central composite design (CCD).

Std.	Run	Coded variables			Actual variables			Biochar yield (%)	O/C ratio	C/N ratio
		A	B	C	A (°C)	B (min)	C (°C min⁻¹)			
1	5	−1	−1	−1	200.00	60.00	5.00	83.92	0.714	–
2	17	+1	−1	−1	600.00	60.00	5.00	35.70	0.295	88.81
3	10	−1	+1	−1	200.00	180.00	5.00	77.66	0.56	–
4	11	+1	+1	−1	600.00	180.00	5.00	37.75	0.221	–
5	14	−1	−1	+1	200.00	60.00	15.00	57.82	0.619	41.40
6	2	+1	−1	+1	600.00	60.00	15.00	31.62	0.204	–
7	15	−1	+1	+1	200.00	180.00	15.00	76.55	0.394	20.10
8	12	+1	+1	+1	600.00	180.00	15.00	35.39	0.28	–
9	1	−α	0	0	63.64	120.00	10.00	95.30	0.579	–
10	20	+α	0	0	736.36	120.00	10.00	32.34	0.438	–
11	16	0	−α	0	400.00	19.09	10.00	42.66	0.282	76.66
12	18	0	+α	0	400.00	220.91	10.00	65.93	0.366	53.08
13	19	0	0	−α	400.00	120.00	1.59	36.59	0.256	124.85
14	6	0	0	+α	400.00	120.00	18.41	48.42	0.276	–
15	7	0	0	0	400.00	120.00	10.00	46.72	0.271	–
16	4	0	0	0	400.00	120.00	10.00	46.72	0.271	–
17	13	0	0	0	400.00	120.00	10.00	46.72	0.271	–
18	9	0	0	0	400.00	120.00	10.00	46.72	0.271	–
19	8	0	0	0	400.00	120.00	10.00	46.72	0.271	–
20	3	0	0	0	400.00	120.00	10.00	46.72	0.271	–

TABLE 3 | Average elemental composition of banana peel biochar as analyzed using energy dispersive X-ray analysis.

Std.	Run	Elemental composition (%)									
		C	O	S	N	P	K	Al	Cl	Mg	Si
1	5	54.45	38.9	0.107	0	0.207	4.587	0.277	1.47	0	0
2	17	63.65	18.76	0.143	0.717	0.473	12.83	0.487	2.373	0.053	0.51
3	10	59.83	33.52	0.183	0	0.237	4.883	0.097	1.19	0	0.06
4	11	68.48	15.16	0	0	0.533	12.59	0.083	2.467	0.15	0.533
5	14	56.72	35.12	0.253	1.37	0.153	4.707	0.113	1.49	0	0.08
6	2	71.33	14.58	0.04	0	0.473	10.25	0	2.663	0.117	0.553
7	15	59.36	23.38	0.197	2.953	0.08	6.273	0.31	1.283	0	0.277
8	12	65.19	18.25	0.143	0	0.67	13.16	0	1.82	0.13	0.633
9	1	59.71	34.56	0.067	0	0.193	4.207	0.267	0.857	0	0.137
10	20	56.83	24.91	0.183	0	0.7	14.3	0.237	2.423	0.227	0.187
11	16	67.72	19.08	0.08	0.883	23.95	9.337	0.27	1.4	0.06	0.66
12	18	64.23	23.52	0.083	1.21	0.393	7.66	0.23	1.273	0.053	1.05
13	19	68.67	17.57	0.073	0.55	0.507	9.653	0.187	2.523	0.053	0.167
14	6	68.10	18.8	0	0	0.363	9.657	0.11	2.643	0.06	0.28
15	7	68.77	18.62	0	0	0.34	9.193	0.48	2.21	0.057	0.333
16	4	68.77	18.62	0	0	0.34	9.193	0.48	2.21	0.057	0.333
17	13	68.77	18.62	0	0	0.34	9.193	0.48	2.21	0.057	0.333
18	9	68.77	18.62	0	0	0.34	9.193	0.48	2.21	0.057	0.333
19	8	68.77	18.62	0	0	0.34	9.193	0.48	2.21	0.057	0.333
20	3	68.77	18.62	0	0	0.34	9.193	0.48	2.21	0.057	0.333

model, in which the experiment is carried out at the same operating conditions for all center points (Behera et al., 2018). The number of center points is typically within a value from 2 to 6. This factorial design approach requires five spaced level for each factor, which are coded as ± α for 2n axial points, 0 for center points, and ±1 for the remaining points. Alpha (α) can be computed using **Eq. 3**, and the value is 1.68719 for experiment involving three factors.

$$\text{Alpha } (\alpha) = \left[2^k\right]^{(1/4)} \tag{3}$$

where k is the number of factors in the experiment.

While the optimum is usually assumed to be within the limits for the area of interest (±1), the alpha value ensures that the extreme axial runs in the experiment are within the area of operability and gives rotatability to the design. Therefore, CCD with set alpha values can be used to predict the response where the manipulated variables are outside of the chosen limits by checking the variance of model prediction through screening analysis and ensuring that the variance is constant at all points equidistant from the center point (Behera et al., 2018). Since the effect of the second order cannot be estimated in a separate manner using 2n factorial design, CCD was employed for modelling this quadratic effect (Behera et al., 2018). The coded factors can be correlated with the actual values of the variables. Hence, regression models for modelling quadratic surface involving the coded factors and the actual levels can both be determined as shown in **Eq. 4** and both can be used to predict the response for given levels of each factor (Choong Lek et al., 2018). The equation with coded factor can be used to make comparison on the factor coefficients to study the relative effect of each factor. Actual value of the response can be predicted using actual equation, where it follows the original units of the factors.

$$Y = \beta_0 + \sum_{i=1}^{n} \beta_i X_i + \sum_{i=1}^{n} \sum_{j=i+1}^{n} \beta_{ij} X_i X_j + \sum_{i=1}^{n} \beta_{ii} X_i^2 \tag{4}$$

where Y is the predicted response; β_0 is the constant; β_i is the linear coefficient; β_{ij} is the interaction coefficient; β_{ii} is the quadratic coefficient; n is the number of factors; and X_i and X_j are the coded or the actual values of the factors respectively.

For modelling the response surface with CCD involving three manipulated variables, 20 runs are required. This is evident as seen from **Eq. 5** used to compute the number of runs required. The contour plot and response surface can be plotted based on the experimental data.

$$N = 2^n + 2n + n_c = 2^3 + 2(3) + 6 = 20 \tag{5}$$

where N is the number of runs required; n is the number of factors; n_c is the number of center points.

Eight factorial points (2^n), six axial points (2n) and six replicates at central points (n_c) conducted at the same operating conditions were used in this CCD design. These points are as seen in **Figure 1**, in which the factorial points are located within distance of 1 from the center points while the axial points are located within distance of α = 1.68719 from the center points. **Equation 4** for experimental design with three factors can be transformed into **Eq. 6**.

Analysis of variance (ANOVA) was conducted to investigate the fit summary and significance of each independent variable as shown in **Eq. 6**.

$$Y = \beta_0 + \beta_1 A + \beta_2 B + \beta_3 C + \beta_4 AB + \beta_5 AC + \beta_6 BC + \beta_7 A^2 + \beta_8 B^2 + \beta_9 C^2 \tag{6}$$

where Y is the predicted response; β_0 is the constant coefficient; β_1 to β_3 are the constant coefficients; β_4 to β_6 are the interaction coefficients; β_7 to β_9 are the quadratic coefficients; and A, B and C

TABLE 4 | Analysis of variance (ANOVA) of CCD model for biochar yield.

Source	Sum of squares	Degrees of freedom	Mean square	F-value	*p*-value	Remarks
Model	6,094.63	9	677.18	19.96	<0.0001	Significant
Temperature (A)	5,002.41	1	5,002.41	147.44	<0.0001	Significant
Residence time (B)	241.47	1	241.47	7.12	0.0236	Significant
Heating rate (C)	13.85	1	13.85	0.4083	0.5372	
AB	5.53	1	5.53	0.1629	0.6950	
AC	53.92	1	53.92	1.59	0.2360	
BC	89.18	1	89.18	2.63	0.1360	
A^2	548.95	1	548.95	16.18	0.0024	Significant
B^2	113.33	1	113.33	3.34	0.0976	
C^2	26.82	1	26.82	0.7904	0.3949	
Residual	339.29	10	33.93			
Lack of fit	339.29	5	67.86			
Pure error	0.0000	5	0.0000			
Total	6,433.92	19				

TABLE 5 | Analysis of variance (ANOVA) of CCD model for O/C ratio.

Source	Sum of squares	Degrees of freedom	Mean square	F-value	*p*-value	Remarks
Model	0.3319	9	0.0369	4.55	0.0134	Significant
Temperature (A)	0.1701	1	0.1701	20.98	0.0010	Significant
Residence time (B)	0.0041	1	0.0041	0.5019	0.4948	
Heating rate (C)	0.0049	1	0.0049	0.6076	0.4537	
AB	0.0181	1	0.0181	2.24	0.1655	
AC	0.0066	1	0.0066	0.8086	0.3897	
BC	0.0008	1	0.0008	0.0962	0.7628	
A^2	0.1225	1	0.1225	15.11	0.0030	Significant
B^2	0.0105	1	0.0105	1.29	0.2823	
C^2	0.0006	1	0.0006	0.0739	0.7912	
Residual	0.0811	10	0.0081			
Lack of fit	0.0811	5	0.0162			
Pure error	0.0000	5	0.0000			
Total	0.4130	19				

are the coded or the actual values of the factors respectively. For actual factors, A is the operating temperature in ˚C, B is the heating rate in $^{\circ}C\ min^{-1}$ and C is the residence time in minute). The coded factors are dimensionless.

Completely Randomized Design

A completely randomized design (CRD) is a relatively simple experimental design, where the subjects are randomly assigned to treatment. It provides a maximum degree of freedom for error. For instance, the analysis of data from CRD can still be carried out even when there is no response in some of the experimental units. The three basic principles of CRD include randomization and replication. This design originated from agricultural application, and it is the most suitable and therefore most commonly used experimental design model for this application. Randomization involves allocating the treatments to the experimental units in a completely random order in order to control the effect of random error. It is assumed that the extraneous variables affect the treatments equally in which significant differences between conditions can be attributed to the independent variables fairly. The replications are the times where the treatment appears in a single experiment. Each treatment has the same number of replications and it is done to further minimize the random error and improves the fitness of the model. Similar with RSM with CCD design, blocking involves the interaction model with another factor. Blocking reduces the experimental error by eliminating the contributions of predicted or known sources of variation, where the experimental units are grouped into blocks (Fao.org., 2020). The conditions within each block are as homogeneous as possible, while large difference may exist between these two blocks. Only one type of biochar was involved and it was assumed that no other factors were involved in this experiment. Therefore, the experiment was assumed to consist of a single block as in typical CRD models.

The number of experimental units required can be calculated easily as in **Eq. 7**, considering five replications to be used. Pot experiment is used for developing the CRD design and the treatments involved in this study are the biochar dosages of 0, 3, 9 and 15 g respectively as shown in **Figure 2** which are independent on each other. The pots are randomly placed to

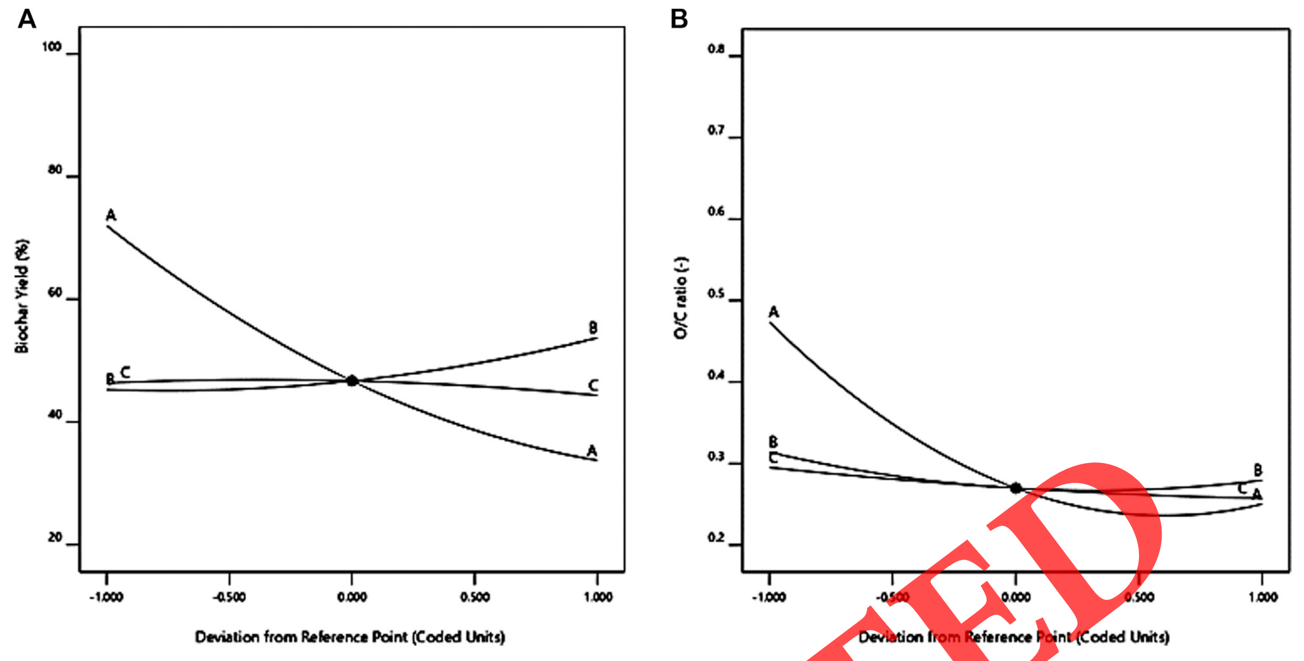

FIGURE 9 | Perturbation plots for **(A)** biochar yield and **(B)** O/C ratio.

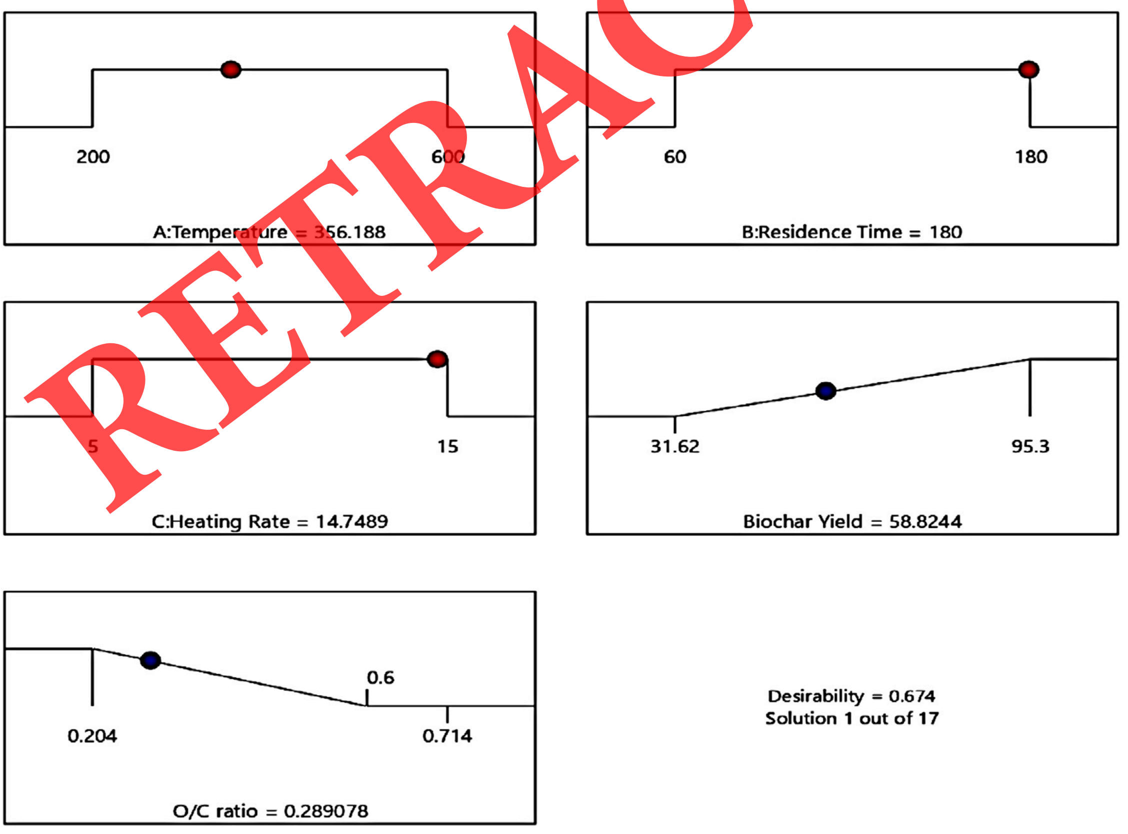

FIGURE 10 | Results from numerical optimization.

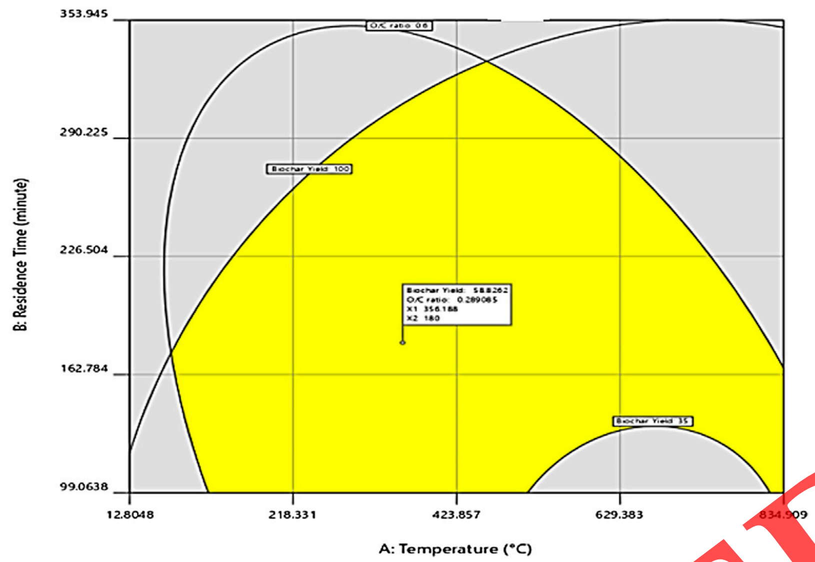

FIGURE 11 | Overlay plot with marked optimization condition, at constant heating rate of 14.74°C·min^{-1}.

eliminate any the effect of any possible external factors that may affect the plant growth.

$$N = n(n_r) = 4(5) = 20 \tag{7}$$

where N is the number of experimental units required; n is the number of treatments; n_r is the number of replications.

The general model of CRD with one factor can be expressed as **Eq. 8** to correlate the factor with the response, Y. This model is further analyzed with analysis of variance (ANOVA) to determine the fitness of the model.

$$Y_{ij} = \mu + \sum_{i=1}^{n} \eta i + e_{ij} \tag{8}$$

where μ is computed mean based on all available experimental subjects; ηi is the constant that shows the effect of ith treatment response; e_{ij} is the error term normally distributed independently with mean of zero and constant variance.

Analysis of Variance

Validity of the central composite design (CCD) and completely randomized design (CRD) were tested using analysis of variance (ANOVA) available in the statistical software Design Expert developed by Stat-Ease, Inc., It defines the interaction between the independent and dependent variables through regression analysis. The significance of the developed model was determined by identifying the F-value while the significance of the model terms was identified through p-values at 95% confidence interval. The best polynomial model was chosen mainly based on the accuracy by checking the coefficient of R^2. Signal to noise ratio of the model was computed by adequacy precision. T-test was also conducted for the CRD model to test the significance of difference between means of each treatment, which are the biochar dosages.

RESULTS AND DISCUSSION

Development of Regression Equation for Biochar Production and Analysis of Variance

The regression analysis of the parameters involving pyrolysis of banana peels to produce biochar was performed using RSM. These parameters were as shown in **Tables 1**, **2**, which showed the range of the operating conditions (independent variables) in actual and coded levels along with the experimental results (response) obtained. The O/C and C/N ratios were obtained based on the results of EDX as demonstrated in **Table 3**. As suggested by the Design-Expert software, quadratic model was best used to correlate the independent variables with the dependant variables and the equations were as shown in **Eqs 9, 10** respectively in terms of coded factors. Coded factors are shown in a scale of −1 to +1 and serves to reduce the magnitude of the actual factors, also known as uncoded factors. This regression model was further tested for its significance and adequacy through ANOVA.

F-value and p-value (probability value) for each model terms were determined to identify their significance as shown in **Tables 4**, **5** respectively. The F-value is the ratio between two variances, while p-value is the probability where results with extreme values than observed values are obtained. Large F-values lead to small p-values (Prob. > F) and indicate that the model terms are significant. In the case of biochar yield, the model has a large F-value of 19.96. When the p-values within 95% confidence interval are less than 0.05, the model terms are considered to be significant. It was found that pyrolysis temperature and residence time had significant impact on the biochar yield, while temperature was the only factor that had significant impact on the O/C ratio of the biochar. The lack of fit in both cases were not significant, implying an overall good model fitting.

TABLE 6 | Analysis of variance (ANOVA) of CRD model for biochar dosage at week 1.

Source	Sum of squares	Degrees of freedom	Mean square	F-value	*p*-value	Remarks
Model	28.85	2	14.43	13.13	0.0011	Significant
Biochar dosage (A)	28.85	2	14.43	13.13	0.0011	Significant
Pure error	13.18	12	1.10			
Total	42.04	14				

TABLE 7 | Analysis of variance (ANOVA) of CRD model for biochar dosage at week 2.

Source	Sum of squares	Degrees of freedom	Mean square	F-value	*p*-value	Remarks
Model	575.69	2	287.85	18.86	0.0002	Significant
Biochar dosage (A)	575.69	2	287.85	18.86	0.0002	Significant
Pure error	183.12	12	15.26			
Total	758.82	14				

TABLE 8 | Analysis of variance (ANOVA) of CRD model for biochar dosage at week 3.

Source	Sum of squares	Degrees of freedom	Mean square	F-value	*p*-value	Remarks
Model	1,002.51	2	501.25	20.22	0.0001	Significant
Biochar dosage (A)	1,002.51	2	501.25	20.22	0.0001	Significant
Pure error	297.47	12	24.79			
Total	1,299.97	14				

TABLE 9 | Analysis of variance (ANOVA) of CRD model for biochar dosage at week 4.

Source	Sum of squares	Degrees of freedom	Mean square	F-value	*p*-value	Remarks
Model	836.70	2	418.35	7.81	0.0066	Significant
Biochar dosage (A)	836.70	2	418.35	7.81	0.0066	Significant
Pure error	638.22	12	53.19			
Total	1,474.92	14				

The O/C ratio model was also significant, with a F-value of 4.55, and there was only a 1.34% chance that an F-value this large can occur due to noise. The coefficient of determination, R^2, signifies the probability in which the response variable (dependent variable) was influenced by explanatory variables (independent variables) and their interactions. The adjusted R^2 value in the biochar yield model was 0.8998 close to 1 and therefore implying that model was suitable for predicting response. For O/C ratio model, the adjusted R^2 value was 0.627, which signifies inaccuracy of the model. Through detailed studies and research, this model can be improved using model transformation, which was not used and discussed in this study. Adequacy precision of the models are 16.0954 and 7.3045 respectively. The adequacy precision of greater than 4 signifies sufficient signal to navigate signal space.

$$\text{Biochar Yield }(\%) = 46.7 - 19.14A + 4.2B - 1.01C - 0.8313AB + 2.6AC + 3.34BC + 6.17A^2 + 2.8B^2 - 1.36C^2 \tag{9}$$

$$O/C\,(\%) = 0.2697 - 0.1116A - 0.0173B - 0.019C + 0.0476AB + 0.0286AC + 0.0099BC + 0.0922A^2 + 0.027B^2 + 0.0064C^2 \tag{10}$$

where A, B and C are the coded values of the factors respectively. A is the operating temperature; B is the residence time and C is the heating rate.

Effect of Temperature, Residence Time and Heating Rate on the Biochar Yield and O/C Ratio of Biochar

The three-factor interaction impact on the biochar yield and O/C ratio of biochar was investigated using response surface. This three-dimensional response surface showed two of the independent variables on the x and y axes and the response was shown on the z-axis. The remaining factor was held constant. The effect of temperature, residence time and heating

TABLE 10 | Biochar dosage and respective mean plant height.

Week	Biochar dosage (%)	Average plant height (cm)
0	0	4.70
	1	4.46
	3	4.12
	5	4.32
1	0	8.26
	1	7.76
	3	5.10
	5	5.96
2	0	23.44
	1	25.72
	3	12.18
	5	—
3	0	29.74
	1	34.08
	3	14.98
	5	—
4	0	33.42
	1	37.04
	3	19.70
	5	—

TABLE 11 | T-test for relationship between biochar dosage and average plant height.

Week	Treatment contrasts	Mean difference	Prob > |t|
1	1 vs. 2	0.5	0.4653
	1 vs. 3	3.16	0.0005
	2 vs. 3	2.66	0.0017
2	1 vs. 2	−2.30	0.3702
	1 vs. 3	11.84	0.0004
	2 vs. 3	14.14	<0.0001
3	1 vs. 2	−4.34	0.1933
	1 vs. 3	14.76	0.0005
	2 vs. 3	19.10	<0.0001
4	1 vs. 2	−3.62	0.4478
	1 vs. 3	13.72	0.0116
	2 vs. 3	17.34	0.0027

rate on biochar yield and O/C ratio are shown in **Figures 3-8**. As shown in **Table 4**, the effect of temperature and residence time was more significant, which was further proven by the response surfaces. Quadratic function of pyrolysis temperature and residence time had similar effect on biochar yield, in which the temperature was the higher-level significance compared with residence time. This is shown where A^2 term is significant while B^2 is not. Response surface showed that lower temperature leads to higher biochar yield. This is due to the higher rate of primary decomposition and devolatilization at higher temperature (Kabir and Hameed, 2017). The heating rate had minimal impact on the biochar yield and O/C ratio of biochar produced. The O/C ratio was mostly governed by the pyrolysis temperature. It was speculated that volatile matter content decreases as the pyrolysis temperature is increased, while the fixed carbon increases. This is due to the higher removal of volatile compounds at higher temperature while more solid combustible residue is being produced which contributes to high fixed carbon content (Zou et al., 2017). Hence, the increasing carbon content causes decrease in O/C ratio of the biochar produced as the pyrolysis temperature increases. The perturbation plots were also plotted as shown in **Figure 9** to show the effect of the independent variables on the responses more clearly.

O/C ratio indicates the degree of carbonation and aromaticity in biomass and biochar, which in turn indicates its interaction with soil (Zainal et al., 2016). These ratios should be as low as possible, in which the value of O/C should be less than 0.4 as it shows a good interaction of the biochar produced with the soil (Zainal et al., 2016). High C/N ratio in biochar is suitable for the soil amendment as it can greatly reduce the N_2O from the soil. C/N ratio also indirectly relates to nitrogen mineralization during biochar-soil microorganism interaction in decomposing organic materials (Zainal et al., 2016). Although the lowest pyrolysis temperature results in the highest biochar yield, the O/C ratio is also the highest. Biochar has an O/C ratio of between 0 to 0.6 and therefore any residue with O/C ratio higher than 0.6 is not considered as biochar (Energies, 2017).

Determination of optimum pyrolysis operating condition was one of the vital parts of this study and was obtained using numerical optimization method. The significance of O/C ratio was set to be higher than the biochar yield as it dictates whether the residue produced is biochar. The optimization results with high desirability was obtained and shown in **Figure 10**. The overlay graph was plotted using a similar concept as perturbation plots, in which two of the manipulated variables are plotted as x and y axes respectively, while using the last manipulated variable with the optimal value as identified as the constant shown in **Figure 11**. The range of desired biochar yield was set to be above 35% and the range of O/C ratio was set to be below 0.6. Highlighted area showed the operating conditions in which the response obtained was within the desired range. The optimum operating conditions for pyrolysis of banana peels biomass were found to be temperature of 356.1°C, residence time of 180 min, and heating rate of 14.7°C·min^{-1}. The biochar yield and O/C ratio of biochar found at these operating conditions were 58.8% and 0.289 respectively.

Effect of Banana Peel Biochar Dosage on the Height of Kangkong Plants

Similar with RSM, the ANOVA using the CRD model examined the effect of percentage of biochar dosage based on total mass of soil on the plant height at each week as shown in **Tables 6–9** respectively. F-value and *p*-value for the model term were determined to identify their significance. The F-value is the ratio between two variances, while *p*-value is the probability where results with extreme values than observed values are obtained. Large F-values lead to small *p*-values (Prob. > F) and indicate that the model terms are significant. The model was simulated for each week and all models had large F-values. When the *p*-values within 95% confidence interval are less than 0.05, the model terms are considered to be significant. This denotes that the model term, biochar dosage, with very small *p*-values was significant. The determination coefficient, R^2, signifies the probability in which the sample variation is

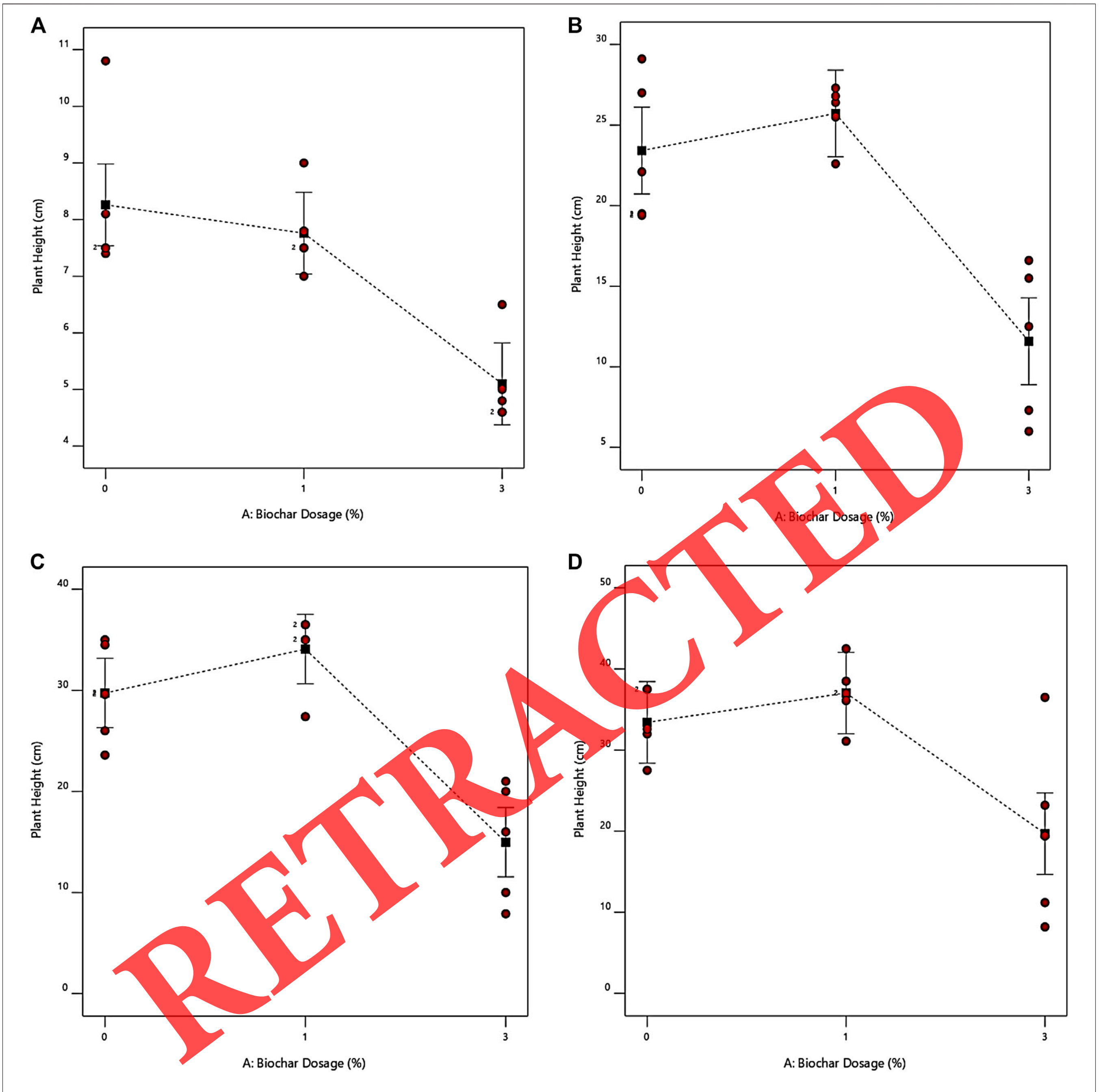

FIGURE 12 | One-factor plot that shows the relationship of biochar dosage and kangkong plant height at **(A)** week 1 **(B)** week 2 **(C)** week 3 and **(D)** week 4 respectively.

attributed to the factors and their interactions. The adjusted R^2 values for all models were close to 1 and therefore implying that the models are suitable for predicting response. Adequacy precision of the models were large enough and signifies sufficient signal to navigate signal space.

The height of the *kangkong* plants were recorded every week until week 4 after germination. Average height of plants using different dosages was then computed each week as shown in **Table 10**. T-test was conducted to determine the significance of the dosage levels on the mean height of kangkong plants and further justify the best biochar dosage for each week. This was done by comparing the mean value of different treatment levels, which are the biochar dosage of 0% (Treatment 1), 1% (Treatment 2), 3% (Treatment 3). A negative mean difference denotes that the mean value of the first treatment is smaller than the second treatment in the treatment contrasts, and vice versa. The significance of the mean difference was justified through the values of Prob > |t| for each treatment contrasts. The values of

Prob > |t| less than 0.05 indicates that the mean difference between the two treatments is significant, while value of greater than 0.1 indicates that the mean difference is not significant. Hence, the best biochar dosage was determined by comparing the mean difference and identifying the biochar dosage that yields the highest plant height on each week. The results of the t-test were as shown in **Table 11**.

On the first week, plants with no biochar dosage had the best growth rate overall. However, the mean difference between plants with no biochar dosage and plants with 1% dosage was not significant, as shown in the high Prob > |t| value of 0.4653. These biochar dosages performed relatively well on the growth of the plants as compared to plants with 3% biochar dosage. 1% biochar dosage yielded the highest plant height on subsequent weeks. Similarly, plant height with 3% biochar dosage was relatively short. Although there was no significant difference between plants 1% biochar dosage and plants without any biochar dosage in the following weeks, the difference was still larger than on the first week, with lower Prob > |t| as evident. Hence, biochar dosage of 1% was chosen as the optimal biochar dosage.

Higher biochar dosages affect the plant growth adversely. This may be due to the alkaline property of the biochar that causes the soil pH to be too high at higher application rate and reduces the precipitation of certain micronutrients such as boron and manganese in the soil (Pandey et al., 2019). The concentration of nitrogen in banana peel biochar was found to be negligible. Hence, the high nitrogen content in soil is prone to being adsorbed by the biochar dosed at high level. The high dosage of biochar also tends to block the pores in the soil and causes the water retention capability to be too high and affects the elongation of roots. The plants with biochar dosage of 5% wilted starting from the second week after germination. Therefore, these were excluded from the CRD model.

The plot that contained all the response data and the average value at each level of the treatment were illustrated as shown in **Figure 12**. It provides an excellent overview of the data and spread of the response due to the effect of the biochar levels of the height of kangkong. 95% confidence interval was considered for each treatment. This is known as one factor effect plot that shows the linear effect when a single factor is changed from (−1) to (+1) levels of the factor. The red dots showed the experimental data points responses. The average values of the data points were connected in a quadratic fashion that shows the relationship between the biochar dosage and plant height.

CONCLUSION

Banana peels biomass proves to be a potential precursor to biochar. This biochar has great potential in agricultural application with the appropriate dosage. In this study, pyrolysis was utilized to convert banana peels biomass into biochar. The operating conditions of the pyrolysis process, namely temperature, residence time and heating rate were altered and the optimum operating condition was determined through analysis of the biochar produced. This biochar was then used in different dosages to test its effect on the growth of *Ipomoea aquatica* plants. The EDX analysis was performed and biochar yield was computed, with the optimum biochar being obtained from slow pyrolysis at pyrolysis temperature of 356.1°C, residence time of 180 min, and heating rate of 14.7°C·min^{-1} with biochar yield and O/C ratio of 58.8% and 0.289, respectively. 1% dosage of the biochar with respect to soil weight yields the highest average *Ipomoea aquatica* plant height which was 37.04 cm. This study shows the potential of using response surface methodology with CCD as the experimental design to obtain the optimal results, as well as CRD to design a pot experiment.

DATA AVAILABILITY STATEMENT

The original contributions presented in the study are included in the article/Supplementary Material, further inquiries can be directed to the corresponding authors.

AUTHOR CONTRIBUTIONS

TZ: Conceptualization, Methodology, Investigation, Data curation, Validation, Visualization, Writing—original draft. KM: Project administration, Investigation, Resources, Software. AnS: Project administration, Supervision. AjS: Resources, Supervision. SA: Software, Review-editing. Y-MC: Funding acquisition, Review-editing. D-VV: Supervision, Project administration. SL: Supervision, Project administration.

REFERENCES

Abu Darhak, R. (2015). Transformation of agricultural sector in Malaysia through agricultural policy. Available at: http://ap.fftc.agnet.org/ap_db.php?id=386&print=1 (Accessed March 13 , 2020).

Behera, S., Meena, H., Chakraborty, S., and Meikap, B. (2018). Application of response surface methodology (RSM) for optimization of leaching parameters for ash reduction from low-grade coal. *Inter. J. Min. Sci. Tech.* 28 (4), 621–629. doi:10.1016/j.ijmst.2018.04.014

Choong Lek, B., Peter, A., Qi Chong, K., Ragu, P., Sethu, V., Selvarajoo, A., et al. (2018). Treatment of palm oil mill effluent (POME) using chickpea (*Cicer arietinum*) as a natural coagulant and flocculant: evaluation, process optimization and characterization of chickpea powder. *J. Env. Chem. Engi.* 6 (5), 6243–6255. doi:10.1016/j.jece.2018.09.038

Chung, C., Selvarajoo, A., Sethu, V., Koyande, A., Arputhan, A., and Lim, Z. (2018). Treatment of palm oil mill effluent (POME) by coagulation flocculation process using peanut-okra and wheat germ-okra. *Clean Technol. Environ. Policy* 20 (9), 1951–1970. doi:10.1007/s10098-018-1619-y

Danish, M., Naqvi, M., Farooq, U., and Naqvi, S. (2015). *Characterization of south Asian agricultural residues for potential utilization in future "energy mix"*. London, United Kingdom: Elsevier Ltd. . Available at: https://www.sciencedirect.com/science/article/pii/S1876610215013727

Diler, E., and Ipek, R. (2012). An experimental and statistical study of interaction effects of matrix particle size, reinforcement particle size and volume fraction on the flexural strength of Al–SiCp composites by P/M using central composite design. *Mater. Sci. Eng. A*. 548, 43–55. doi:10.1016/j.msea.2012.03.066

Eia.gov (2020). Biomass explained - U.S. Energy information administration (EIA). Available at: https://www.eia.gov/energyexplained/biomass/ (Accessed March 17 , 2020).

Energies (2017). Effect of temperature on the structural and physicochemical properties of biochar with apple tree branches as feedstock material. *Energies* 10 (9), 1293. doi:10.3390/en10091293

Fao.org. (2020). A statistical manual for forestry research. Available at: http://www.fao.org/3/X6831E/X6831E07.htm (Accessed March 13 , 2020).

Itl.nist.gov. (2020). Central composite designs (CCD). Available at: https://www.itl.nist.gov/div898/handbook/pri/section3/pri3361.htm (Accessed March 27 , 2020)

Kabenge, I., Omulo, G., Banadda, N., Seay, J., Zziwa, A., and Kiggundu, N. (2018). *Characterization of banana peels wastes as potential slow pyrolysis feedstock*. Richmond Hill, ON: Canadian Center of Science and Education. Available at: https://www.researchgate.net/publication/324119052_Characterization_of_Banana_Peels_Wastes_as_Potential_Slow_Pyrolysis_Feedstock.

Kabir, G., and Hameed, B. H. (2017). Recent progress on catalytic pyrolysis of lignocellulosic biomass to high-grade bio-oil and bio-chemicals. *Renew. Sustain. Energy Rev.* 70, 945–967. doi:10.1016/j.rser.2016.12.001

Lawal, A., Hassan, M., Farid, M., Yasim-Anuar, T., Yusoff, M., Zakaria, M., et al. (2020). Production of biochar from oil palm frond by steam pyrolysis for removal of residual contaminants in palm oil mill effluent final discharge. *J. Clean. Prod.* 265, 121643. doi:10.1016/j.jclepro.2020.121643

Lee, X., Lee, L., Gan, S., Thangalazhy-Gopakumar, S., and Ng, H. (2017). Biochar potential evaluation of palm oil wastes through slow pyrolysis: thermochemical characterization and pyrolytic kinetic studies. *Bioresour. Technol.* 236, 155–163. doi:10.1016/j.biortech.2017.03.105

Montogomery, D. C. (2014). *Design and analysis of experiments*. 8th Edn. New York, NY: John Wiley & Sons.

Morin, M., Pécate, S., Hémati, M., and Kara, Y. (2016). Pyrolysis of biomass in a batch fluidized bed reactor: effect of the pyrolysis conditions and the nature of the biomass on the physicochemical properties and the reactivity of char. *J. Anal. Appl. Pyrol.* 122, 511–523. doi:10.1016/j.jaap.2016.10.002

Nanda, S., Mohanty, P., Pant, K., Naik, S., Kozinski, J., and Dalai, A. (2014). *Characterization of North American lignocellulosic biomass and biochars in terms of their candidacy for alternate renewable fuels*. New York, NY: Springer Science+Business Media New York. Available at: https://link.springer.com/article/10.1007/s12155-012-9281-4.

Nbs2020.gov.my (2019). Types of biomass in Malaysia. Available at: https://www.nbs2020.gov.my/biomass-in-malaysia (Accessed April 4 , 2020).

Olawoye, B. (2016). *A comprehensive handout ON central composite design (CCD)*. Ife, Nigeria: Obafemi Awolowo University.

Osman, N., Shamsuddin, N., and Uemura, Y. (2016). Activated carbon of oil palm empty fruit bunch (EFB); core and shaggy. *Proc. Eng.* 148, 758–764. doi:10.1016/j.proeng.2016.06.610

Pandey, H., Pandey, P., Pokhrel, S., and Mandal, R. (2019). Relationship between soil properties and forests carbon: case of three community forests from far Western Nepal. *Bank* 29 (1), 43–52. doi:10.3126/banko.v29i1.25154

Pathak, P., Mandavgane, S., and Kulkarni, B. (2017). Fruit peel waste: characterization and its potential uses. Available at: https://www.researchgate.net/publication/313839639_Fruit_peel_waste_Characterization_and_its_potential_uses.

Rodriguez, J., Lustosa Filho, J., Melo, L., de Assis, I., and de Oliveira, T. (2020). Influence of pyrolysis temperature and feedstock on the properties of biochars produced from agricultural and industrial wastes. *J. Anal. Appl. Pyrol.* 149, 104839. doi:10.1016/j.jaap.2020.104839

Selvarajoo, A., Muhammad, D., and Arumugasamy, S. (2019). An experimental and modelling approach to produce biochar from banana peels through pyrolysis as potential renewable energy resources. *Model. Earth Syst. Environ.* 6 (1), 115–128. doi:10.1007/s40808-019-00663-2

Sial, T., Khan, M., Lan, Z., Kumbhar, F., Ying, Z., Zhang, J., et al. (2019). Contrasting effects of banana peels waste and its biochar on greenhouse gas emissions and soil biochemical properties. *Process Saf. Environ. Protect.* 122, 366–377. doi:10.1016/j.psep.2018.10.030

Suman, S., and Gautam, S. (2018). Biochar derived from agricultural waste biomass act as a clean and alternative energy source of fossil fuel inputs. *Ener. Sys. Env.* doi:10.5772/intechopen.73833

Tan, C. (2014). Local bananas: a cheat sheet on the common banana types sold here. *The Straits Times*. Available at: https://www.straitstimes.com/world/africa/local-bananas-a-cheat-sheet-on-the-common-banana-types-sold-here (Accessed April 4 , 2020).

V Birtwistle, J. (2003). "Dust explosions," in SAChE workshop, Baton Rouge, LA, September 29–30, 2003.

Veiga, P., Schultz, J., Matos, T., Fornari, M., Costa, T., Meurer, L., et al. (2020). Production of high-performance biochar using a simple and low-cost method: optimization of pyrolysis parameters and evaluation for water treatment. *J. Anal. Appl. Pyrol.* 148, 104823. doi:10.1016/j.jaap.2020.104823

Xie, S., Yu, G., Li, C., Li, J., Wang, G., Dai, S., et al. (2020). Treatment of high-ash industrial sludge for producing improved char with low heavy metal toxicity. *J. Anal. Appl. Pyrol.* 150, 104866. doi:10.1016/j.jaap.2020.104866

Zainal, H., Loh, S., and Bachmann, R. (2016). *Production and Characterization of Biochar from palm kernel shell (PKS). J. Oil Palm Res.* Available at: https://www.researchgate.net/publication/312156025_Production_and_Characterization_of_Biochar_from_Palm_Kernel_Shell_PKS.

Zou, C., Wang, C., Liu, H., Wang, H., and Zhang, Y. (2017). Effect of volatile and ash contents in coal on the volatilization of arsenic during isothermal coal combustion. *Energy Fuels* 31 (11), 12831–12838. doi:10.1021/acs.energyfuels.7b02187